

ESTIMATION OF MULTIPATH PROPAGATION PARAMETERS FROM MEASURED CHANNEL DATA

Alle-Jan van der Veen, V.T. Phong Pham and Ramjee Prasad

Delft University of Technology, Dept. Electrical Engineering, 2628 CD Delft, The Netherlands

An antenna array at the base station can be used for mobile source localization and to unravel multipath propagation structures in terms of angles and delays. A recently proposed technique for this purpose is the SIJADE algorithm. We extend this algorithm to a hexagonal array and apply it to measured indoor channel data.

I. INTRODUCTION

Source localization is one of the recurring problems in electrical engineering. In mobile communications, source localization by the base station is of interest for advanced handover schemes, emergency localization, and potentially many user services for which a GPS receiver is impractical. In a multipath scenario, localization involves the estimation of the directions and relative delays of the dominant multipath rays. It is often assumed that the directions and delays of the paths do not change quickly, as fading affects only their powers, so that it makes sense to estimate these parameters. The angle-delay parameters are also essential for space-time selective transmission in the downlink, especially in FDD systems.

Several algorithms for joint high-resolution estimation of multipath angles and delays have recently been introduced in the literature [1–3]. These methods are based on the fact that temporal shifts map to phase shifts in the frequency domain.

In this paper, we will use the “shift-invariance joint angle-delay estimation” (SIJADE) algorithm from [3], which estimates the phase shifts using a multi-dimensional ESPRIT type algorithm. It is applicable if we have an estimated channel impulse response and assume linearly modulated sources with a known pulse shape function and no appreciable doppler shifts. We further assume a multipath model consisting of discrete rays, each parameterized by a delay, complex amplitude (fading), and angle. Accurate results are only possible if the data received by the antennas is sampled at or above the Nyquist rate.

We apply the SIJADE algorithm to a measured indoor channel impulse response at 2.4 GHz and with bandwidth 500 MHz, which was obtained using a 6 element hexagonal antenna array.

II. DATA MODEL

Assume we transmit a digital sequence $\{s_k\}$ over a linear channel, and measure the response using M antennas. The noiseless received data in general has the form $\mathbf{x}(t) = \sum s_k \mathbf{h}(t - kT)$. A

commonly used multiray propagation model, for specular multipath, writes the $M \times 1$ channel impulse response as

$$\mathbf{h}(t) = \sum_{i=1}^r \mathbf{a}(\alpha_i) \beta_i g(t - \tau_i),$$

where $g(t)$ is a known pulse shape function by which $\{s_k\}$ is modulated. In this model, there are r distinct propagation paths, each parameterized by $(\alpha_i, \tau_i, \beta_i)$, where α_i is the direction of arrival (DOA) at the antenna array, τ_i is the path delay, and $\beta_i \in \mathbf{C}$ is the complex path attenuation (fading). The vector-valued function $\mathbf{a}(\alpha)$ is the array response vector to a signal from direction α . Several techniques are available to estimate $\mathbf{h}(t)$, e.g., using training sequences, blind channel estimation, or a channel sounder.

The delay estimation algorithm is based on the properties that in the frequency domain, (1) a delay is mapped into a phase shift, (2) convolution by the known pulse shape function $g(t)$ becomes a pointwise multiplication which is easily inverted on its nonzero support. Thus let us assume that the channel data is available in the frequency domain as a matrix

$$H = [\tilde{\mathbf{h}}(f_{\min}) \quad \tilde{\mathbf{h}}(f_{\min} + \Delta_f) \quad \cdots \quad \tilde{\mathbf{h}}(f_{\max})].$$

If we have M antennas and N samples in frequency domain spaced at Δ_f , then H has size $M \times N$. We also assume that the channel has been sampled at or above the Nyquist rate determined by $g(t)$ so that no aliasing has occurred, and that the influence of $g(t)$ has subsequently been removed by deconvolution (see [3] for details). Then we can write the resulting data model in the frequency domain as $H = ABF$, where

$$A = [\mathbf{a}(\alpha_1) \quad \cdots \quad \mathbf{a}(\alpha_r)], \quad B = \text{diag}(\beta_i)$$

$$F_N = \begin{bmatrix} 1 & \phi_1 & \phi_1^2 & \cdots & \phi_1^{N-1} \\ \vdots & \vdots & & & \vdots \\ 1 & \phi_r & \phi_r^2 & \cdots & \phi_r^{N-1} \end{bmatrix}, \quad \phi_i := e^{-j2\pi\Delta_f\tau_i}$$

(we usually omit the size index of F).

If $r \leq M, N$, then it is possible to estimate the ϕ_i 's and hence the τ_i 's from the shift-invariance structure of F , independent of the structure of A , which is essentially the ESPRIT algorithm. To estimate the DOAs as well, we need to know the array manifold structure. In general, the number of antennas is not large enough to satisfy $M > r$. This problem is avoided by constructing a Hankel matrix out of H .

III. JOINT DELAY AND ANGLE ESTIMATION

A. Algorithm outline

Our objective is to estimate $\{(\alpha_i, \tau_i)\}$ from the shift-invariance properties present in the data model $H = ABF$. For simplicity, let us first assume that our antenna array is a uniform linear array consisting of M omnidirectional antennas spaced at a distance of Δ wavelengths. For an integer $2 \leq m \leq N$, define

$$\Theta = \text{diag}[\theta_1 \cdots \theta_r], \quad A = \begin{bmatrix} 1 & \cdots & 1 \\ \theta_1 & \cdots & \theta_r \\ \vdots & & \vdots \\ \theta_1^{M-1} & \cdots & \theta_r^{M-1} \end{bmatrix}, \quad \theta_i = e^{j2\pi\Delta\sin\alpha_i}$$

$$\Phi = \text{diag}[\phi_1 \cdots \phi_r], \quad A_\phi = \begin{bmatrix} 1 & \cdots & 1 \\ \phi_1 & \cdots & \phi_r \\ \vdots & & \vdots \\ \phi_1^{m-1} & \cdots & \phi_r^{m-1} \end{bmatrix}, \quad \phi_i = e^{-j2\pi\Delta_f\tau_i}$$

If we now construct a block-Hankel matrix $\mathcal{H} : mM \times (N-m+1)$ from equal-sized submatrices of H as

$$\mathcal{H} = \begin{bmatrix} H^{(1)} \\ \vdots \\ H^{(m)} \end{bmatrix}, \quad H^{(i)} := \begin{bmatrix} H_{1,i} \cdots H_{1,N-m+i} \\ \vdots \\ H_{M,i} \cdots H_{M,N-m+i} \end{bmatrix},$$

then it is straightforward to show that \mathcal{H} has a factorization

$$\mathcal{H} = \mathcal{A}BF = \begin{bmatrix} A \\ A\Phi \\ \vdots \\ A\Phi^{m-1} \end{bmatrix} BF.$$

The parameter m should be used to ensure that \mathcal{H} is a rank-deficient matrix (this puts a limit on the number of rays that can be estimated).

The algorithm proceeds by estimating the column span of \mathcal{H} , which is equal to the column span of \mathcal{A} provided F is full rank. Note that $\mathcal{A} = (A_\phi \diamond A)$, where \diamond denotes a column-wise Kronecker product. The estimation of Φ and Θ from the column span of \mathcal{H} is based on exploiting the various shift-invariant structures present in $A_\phi \diamond A$. Define selection matrices

$$\begin{aligned} J_{x\phi} &:= [I_{m-1} \ 0_1] \otimes I_M, & J_{x\theta} &:= I_m \otimes [I_{M-1} \ 0_1], \\ J_{y\phi} &:= [0_1 \ I_{m-1}] \otimes I_M, & J_{y\theta} &:= I_m \otimes [0_1 \ I_{M-1}], \end{aligned}$$

and let $X_\phi = J_{x\phi}\mathcal{H}$, $Y_\phi = J_{y\phi}\mathcal{H}$, $X_\theta = J_{x\theta}\mathcal{H}$, $Y_\theta = J_{y\theta}\mathcal{H}$. These data matrices have the structure

$$\begin{cases} X_\phi = A'BF \\ Y_\phi = A'\Phi BF \end{cases} \quad \begin{cases} X_\theta = A''BF \\ Y_\theta = A''\Theta BF \end{cases} \quad (1)$$

where $A' = J_{x\phi}A$, $A'' = J_{x\theta}A$. If dimensions are such that these are low-rank factorizations, then we can apply the 2-D ESPRIT algorithm [4, 5] to estimate Φ and Θ . In particular, since

$$\begin{aligned} Y_\phi - \lambda X_\phi &= A'[\Phi - \lambda I_r]BF \\ Y_\theta - \lambda X_\theta &= A''[\Theta - \lambda I_r]BF \end{aligned}$$

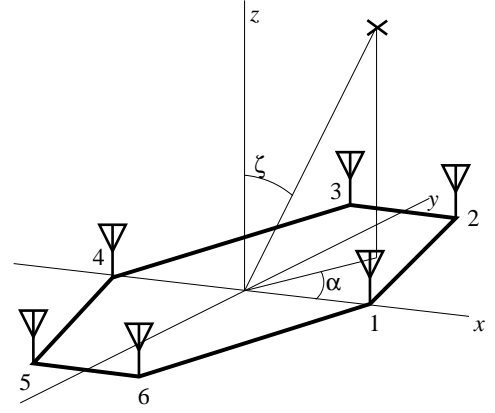


Figure 1. Hexagonal array

the ϕ_i are given by the rank reducing numbers of the pencil (Y_ϕ, X_ϕ) , whereas the θ_i are the rank reducing numbers of (Y_θ, X_θ) . These are the same as the nonzero eigenvalues of $X_\phi^\dagger Y_\phi$ and $X_\theta^\dagger Y_\theta$. (\dagger denotes the Moore-Penrose pseudo-inverse.)

The correct pairing of the ϕ_i with the θ_i follows from the fact that $X_\phi^\dagger Y_\phi$ and $X_\theta^\dagger Y_\theta$ have the same eigenvectors, which is caused by the common factor F . In particular, there is an invertible matrix V which diagonalizes both $X_\phi^\dagger Y_\phi$ and $X_\theta^\dagger Y_\theta$. Various algorithms have been derived to compute such joint diagonalizations. Omitting further details, we propose to use the diagonalization method in [4], although the algorithm in [5] can be used as well. As in ESPRIT, the actual algorithm has an intermediate step in which \mathcal{H} is reduced to its r -dimensional principal column span, and this step will form the main computational bottleneck.

This constitutes the basic SIJADE algorithm [3].

B. Data extension

Since the eigenvalues (ϕ_i, θ_i) are on the unit circle and the array is symmetric, we can double the dimension of \mathcal{H} by forward-backward averaging. In particular, let J denote the exchange matrix which reverses the ordering of rows, and define

$$\mathcal{H}_e = [\mathcal{H} \ J\mathcal{H}^{(c)}], \quad mM \times 2(N-m+1),$$

where (c) indicates taking the complex conjugate. Since $J\mathcal{A}^{(c)} = \mathcal{A}\Phi^{-(m-1)}\Theta^{-(M-1)}$, it follows that \mathcal{H}_e has a factorization

$$\mathcal{H}_e = \mathcal{A}B_e F_e = \mathcal{A}[BF, \Phi^{-m+1}\Theta^{-M+1}B^{(c)}F^{(c)}].$$

The computation of Φ and Θ from \mathcal{H}_e proceeds as before.

C. Hexagonal array

The SIJADE algorithm is readily extended to joint delay plus both azimuth and elevation estimation using a two-dimensional antenna array. In particular, we consider here a uniform hexagonal array with radius R (figure 1). A multipath ray from direction (ζ, α) generates at the i -th antenna a phase lead (with reference to the array center)

$$\phi_i = \frac{2\pi R}{\lambda} [\cos(i-1)\frac{\pi}{3} \quad \sin(i-1)\frac{\pi}{3}] \begin{bmatrix} \sin(\zeta) \cos(\alpha) \\ \sin(\zeta) \sin(\alpha) \end{bmatrix}.$$

The algorithm below will estimate, for each multipath component, the phase differences $\varphi_{21} = \varphi_2 - \varphi_1$, $\varphi_{32} = \varphi_3 - \varphi_2$, and $\varphi_{43} = \varphi_4 - \varphi_3$.

The algorithm starts again with a data matrix H , which simply stacks the frequency responses at the antennas in a $6 \times N$ matrix: $H = ABF$. We construct a Hankel matrix \mathcal{H} by m horizontal shifts, which gives the model $\mathcal{H} = \mathcal{A}BF$ where $\mathcal{A} = A_0 \diamond A$. Extension by forward-backward averaging is still possible: since the array is centro-symmetric, we can define

$$J'' = \begin{bmatrix} 0_{3 \times 3} & I_3 \\ I_3 & 0_{3 \times 3} \end{bmatrix}$$

so that $J''A^{(c)} = A$, assuming zero phase at the center of the array. As before, we set

$$\mathcal{H}_e = [\mathcal{H} \quad J'\mathcal{H}^{(c)}], \quad J' = J \diamond J''.$$

The difference is in the definition of the selection matrices. There are 9 different baselines, but we will not use all of them. The baseline block pairs which we consider are defined by¹

$$\begin{aligned} \mathbf{a}_{x1} &= \begin{bmatrix} a_1 \\ a_5 \end{bmatrix}, \quad \mathbf{a}_{y1} = \begin{bmatrix} a_2 \\ a_4 \end{bmatrix}, & \mathbf{a}_{x2} &= \begin{bmatrix} a_2 \\ a_6 \end{bmatrix}, \quad \mathbf{a}_{y2} = \begin{bmatrix} a_3 \\ a_5 \end{bmatrix}, \\ \mathbf{a}_{x3} &= \begin{bmatrix} a_3 \\ a_1 \end{bmatrix}, \quad \mathbf{a}_{y3} = \begin{bmatrix} a_4 \\ a_6 \end{bmatrix} \end{aligned}$$

and this defines corresponding (2×6) selection matrices J_{x1} etc. For a single multipath component, the shift-invariance structure gives

$$\begin{aligned} \mathbf{a}_{y1} &= \mathbf{a}_{x1} \theta_{21}, & \theta_{21} &= e^{j\varphi_{21}} \\ \mathbf{a}_{y2} &= \mathbf{a}_{x2} \theta_{32}, & \theta_{32} &= e^{j\varphi_{32}} \\ \mathbf{a}_{y3} &= \mathbf{a}_{x3} \theta_{43}, & \theta_{43} &= e^{j\varphi_{43}} \end{aligned}$$

where φ_{ij} is the phase difference between antennas i and j . For multiple components, we similarly obtain $A_{yi} = A_{xi} \Theta_{i+1,i}$, etc., where $\Theta_{i+1,i}$ is a diagonal matrix.

Along with a selection matrix for Φ , we finally obtain 4 coupled matrix pencils from submatrices of \mathcal{H}_e , with structure

$$\begin{cases} X_\phi &= A'BF \\ Y_\phi &= A'\Phi BF \end{cases} \quad \begin{cases} X_{\theta_1} &= A''BF \\ Y_{\theta_1} &= A''\Theta_{21}BF \end{cases} \\ \begin{cases} X_{\theta_2} &= A'''BF \\ Y_{\theta_2} &= A'''\Theta_{32}BF \end{cases} \quad \begin{cases} X_{\theta_3} &= A''''BF \\ Y_{\theta_3} &= A''''\Theta_{43}BF \end{cases}$$

The parameter quadruples $\{(\phi_i, \theta_{21}, \theta_{32}, \theta_{43})\}$ are given by the rank-reducing numbers of each of the pencils, and they are coupled because they all have the same right eigenvectors. This problem is solved as before.

Once the parameter quadruples have been obtained, we can solve the overdetermined system

$$\frac{2\pi R}{\lambda} \begin{bmatrix} -1 & 1 \\ -1 & 1 \\ -1 & -1 \end{bmatrix} \begin{bmatrix} \cos(0) & \sin(0) \\ \cos(\frac{\pi}{3}) & \sin(\frac{\pi}{3}) \\ \cos(\frac{2\pi}{3}) & \sin(\frac{2\pi}{3}) \end{bmatrix} \begin{bmatrix} \sin(\zeta) \cos(\alpha) \\ \sin(\zeta) \sin(\alpha) \end{bmatrix} = \begin{bmatrix} \varphi_{21} \\ \varphi_{32} \\ \varphi_{43} \end{bmatrix}$$

¹The longer baselines 1–3 etc. are omitted because in our application they are larger than $\lambda/2$ which leads to aliasing and related small complications.

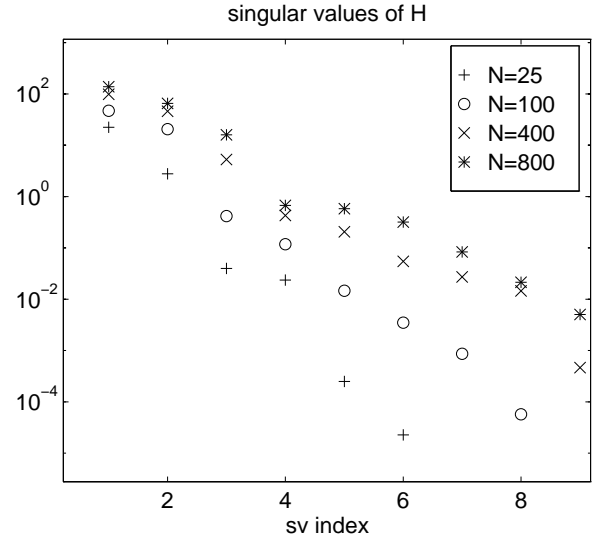


Figure 2. Singular values of \mathcal{H}_e , two rays, no noise.

This gives an estimate for the vector $\mathbf{x} = \begin{bmatrix} \sin(\zeta) \cos(\alpha) \\ \sin(\zeta) \sin(\alpha) \end{bmatrix}$ from

which we estimate ζ and α as

$$\sin(\zeta) = \|\mathbf{x}\|, \quad \tan(\alpha) = \frac{x_2}{x_1}$$

Because the system is overdetermined, we also obtain an idea about the accuracy of these directions.

The number of rays that can be estimated is limited by $r \leq 2m$ and $r \leq 2(N-m+1)$. With forward-backward averaging, we can have at most two rays with equal delays.

IV. EXPERIMENTAL DATA

Our aim is to apply the SIJADE algorithm to experimental indoor channel data at 2.4 GHz, measured in an office at FELTNO (The Hague, The Netherlands) [6]. This office has dimensions 5.6m \times 5.0m, and height 3.5m, and has various metallic objects in it. The measurement set-up consists of a transmit antenna (biconical horn) in the center of the room at a height of 3.0m, and a receiving antenna cluster located at a height of 1.5m and a horizontal distance of 1.1m to the transmitter. The cluster is a hexagonal array with six wideband antennas spaced at $R = 0.0625$ m (approximately $0.5\lambda_c$). The measurement data is 801 frequency-domain samples from a channel sounder, spanning the band 2.15–2.65 GHz. Thus, the spacing between two samples is $\Delta_f = 0.625$ MHz, and the total bandwidth is 500 MHz, corresponding to a time resolution of 2 ns. Since we have frequency-domain channel data, it can directly be used to construct a data matrix H : no Fourier transform is necessary.

A. Applicability of the SIJADE algorithm

There are several issues that limit the applicability of the SIJADE algorithm in the present scenario.

- The frequency band of 500 MHz is rather wide. The angle model is not precisely valid because the wavelength varies

significantly along the band, from 0.14m to 0.11m. If the full band is used, then $\mathbf{a}(\theta, f_{\min}) \neq \mathbf{a}(\theta, f_{\max})$, and the data matrix will not be low rank, even if there would be only a single discrete path. There is also a problem in translating a phase shift into an angle. Thus, for the benefit of direction estimation it would be necessary to run the algorithm on a much smaller band, say 62.5 MHz (101 samples). This reduces the temporal resolution by the same factor, from 2 ns to 16 ns (or from 60 cm to almost 5 m). But at this resolution, many paths have approximately the same delay.

- If forward-backward averaging (conjugation) is used, then we can resolve at most two paths that have approximately the same delay.
- From the rank of the Hankel matrix \mathcal{H}_e , it appears that there are many paths ($r \gg 10$). In fact, the number of paths is hard to tell from the rank, because of the wide-band problem mentioned above.
- If we take the shifts in the Hankel matrix over only 1 sample ($\Delta_f = 0.625$ MHz), then we can estimate delays of up to 1.6 μ s. However, the extent of the impulse response is less than 0.1 μ s, which means that all eigenvalues ϕ_k would be close to 1 and almost the same. An improved resolution is obtained by taking larger shifts, e.g., over 16 samples. If the shift is taken too large, then aliasing will occur.
- Because of the planar array configuration, the array cannot distinguish between rays from above and rays from below.

B. Synthetic data

To test the applicability of the algorithm, we first try it on synthetic data. We take $r = 2$ well-separated rays, with parameters $(\tau, \alpha, \zeta) = (10\text{ns}, 10^\circ, 4^\circ)$ and $(20\text{ns}, 100^\circ, 80^\circ)$. There is no noise. The singular values of \mathcal{H}_e , with parameters $m = 2$ and shift = 16, are shown in figure 2, for varying number of samples N . It is seen that if more than about 100 samples are taken (bandwidth larger than about 60 MHz), the gap between the two large singular values and the others becomes rather small, and detection of the number of rays is not possible. Even with $N = 100$, the gap is less than 2 orders of magnitude. This will eventually limit the total number of rays that can be estimated.

For the 2-ray case, the accuracy of the estimated parameters turns out to be quite good for any N , although the delay estimation improves slightly for larger N . It is more interesting to look at the accuracy for a larger number of rays. Figure 3 and table 1 show the singular values and estimated parameters for synthetic data with 8 rays. Two of the delays have been chosen close. It is seen that if N is small, the temporal resolution is not sufficient and the algorithm gets confused, also for the angle estimates. For $N = 400$ or more, all parameters are estimated quite accurately. However, as seen from the singular value plots, it is almost futile to estimate the total number of incoming rays.

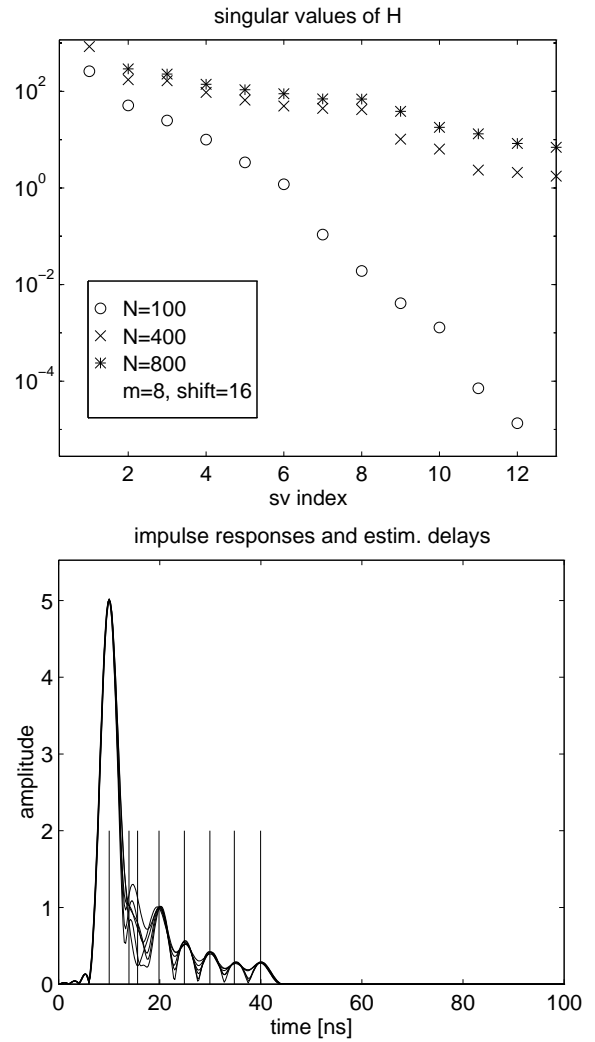


Figure 3. Synthetic data with 8 rays, no noise. (a) Singular values of \mathcal{H}_e . (b) Impulse response and estimated delays.

Table 1. Estimated parameters, synthetic data, varying N

τ [ns]	α [deg]	ζ [deg]
<i>true</i>	<i>true</i>	<i>true</i>
10.0 14.0 16.0 20.0 25.0 30.0 35.0 40.0	10.0 40.0 80.0 100.0 150.0 -20.0 -50.0 -100.0	20.0 80.0 40.0 60.0 30.0 70.0 25.0 85.0
100	10.1 38.0 135.0 110.2 -104.5 -19.3 -57.6 -97.7	19.8 57.4 10.7 72.8 90.0 78.1 22.6 66.0
400	9.9 39.6 72.1 99.2 148.2 -19.3 -47.5 -100.2	20.0 72.3 37.9 60.2 29.9 72.5 25.6 90.0
800	9.9 39.3 69.1 103.5 149.9 -20.2 -49.7 -99.8	20.0 72.7 42.5 53.5 30.2 70.4 24.6 84.8

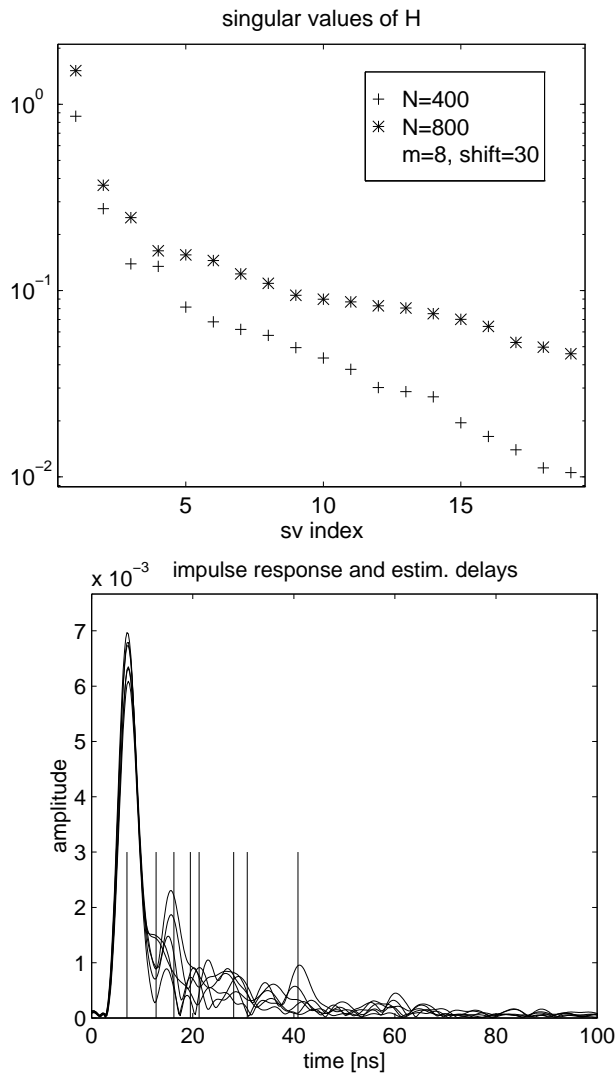


Figure 4. Actual data

Table 2. Estimated parameters, actual data

τ [ns]									
$r = 4$	7.0	13.2	17.9	19.8	-	-	-	-	-
6	7.0	12.8	16.3	19.7	21.4	29.7	-	-	-
8	7.0	12.8	16.3	19.5	21.3	28.1	30.8	40.8	-
α [deg]									
$r = 4$	61.2	53.5	104.2	31.9	-	-	-	-	-
6	61.0	55.3	110.5	42.4	-91.6	-45.0	-	-	-
8	61.3	54.4	110.5	42.2	-96.9	95.1	-154.9	175.3	-
ζ [deg]									
$r = 4$	38.6	36.2	70.9	49.9	-	-	-	-	-
6	38.6	41.7	59.2	47.0	66.2	70.2	-	-	-
8	39.2	38.6	60.1	45.8	74.6	25.4	54.6	32.8	-

C. Actual data

Now that we have seen that in principle it should be possible to estimate the parameters of up to 8 rays, we try the algorithm on actual data. Figure 4 shows the measured impulse responses and singular value plots, and table 2 lists the estimated parameters for $N = 400$ samples, $m = 8$ shifts over 30 samples, and

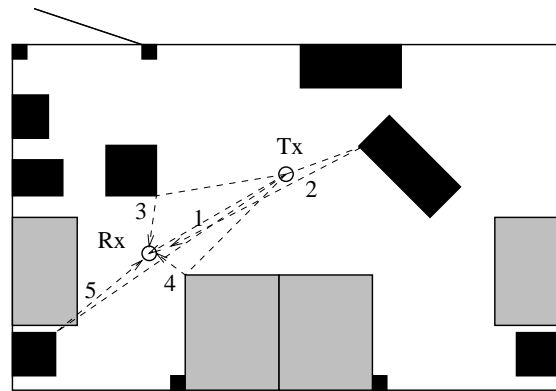


Figure 5.

varying assumed number of rays. The singular values show that there is one strong ray and 3 other significant rays, followed by a slew of other rays that cannot be distinguished from the rank increase caused by the wide-band nature of the data. The estimated parameters of the first 4 or 5 dominant rays do not vary much with changing the number of assumed rays r , so they can be considered to have been estimated fairly accurately. Estimating more rays turns out to be rather unsuccessful, as the results change with varying r , m and N .

We can try to match the estimated parameters to the actual room configuration. Only for the line-of-sight, pertinent data is available: a reported horizontal distance of approximately 1.1m and a vertical distance of 1.5m, leading to a delay of $\tau = 6.2\text{ns}$ and $\zeta = 36^\circ$. Thus, the estimated parameters for the first ray are not too far off. The azimuthal angle of the first ray is not known, but using the estimated angle as a reference, the subsequent rays can be traced back to various metallic objects in the room (two cupboards, a table and a support column), although this part is rather speculative for lack of accurate room geometrics.

REFERENCES

- [1] J. Gunther and A.L. Swindlehurst, "Algorithms for blind equalization with multiple antennas based on frequency domain subspaces," in *Proc. IEEE ICASSP*, vol. 5, (Atlanta (GA)), pp. 2421–2424, 1996.
- [2] M. Wax and A. Leshem, "Joint estimation of directions-of-arrival and time-delays of multiple reflections of known signal," *IEEE Tr. Signal Proc.*, vol. 45, Oct. 1997.
- [3] A.J. van der Veen, M.C. Vanderveen, and A. Paulraj, "Joint angle and delay estimation using shift-invariance techniques," *IEEE Tr. Signal Processing*, vol. 46, Feb. 1998.
- [4] A.J. van der Veen, P.B. Ober, and E.F. Deprettere, "Azimuth and elevation computation in high resolution DOA estimation," *IEEE Trans. Signal Processing*, vol. 40, pp. 1828–1832, July 1992.
- [5] M.D. Zoltowski, M. Haardt, and C.P. Mathews, "Closed-form 2-D angle estimation with rectangular arrays in element space or beamspace via Unitary ESPRIT," *IEEE Trans. Signal Processing*, vol. 44, pp. 316–328, Feb. 1996.
- [6] G.J.M. Janssen and R. Prasad, "Propagation measurements in an indoor radio environment at 2.4 GHz, 4.75 GHz and 11.5 GHz," in *42nd VTS Conference*, (Denver), pp. 617–620 vol.2, IEEE, 1992.